9858 *Biochemistry* **2010,** *49,* 9858–9865
DOI: 10.1021/bi101415w

BIOCHEMISTRY
including biophysical chemistry & molecular biology
Article

Novel Fatty Acid Acylation of Lens Integral Membrane Protein Aquaporin-0[†]

Kevin L. Schey,*[,‡] Danielle B. Gutierrez,[§] Zhen Wang,[‡] Junhua Wei,[‡] and Angus C. Grey[‡,∥]

[‡]*Department of Biochemistry, Vanderbilt University, Nashville, Tennessee 37232, United States, and*
[§]*Department of Pharmacology, Medical University of South Carolina, Charleston, South Carolina 29425, United States*
[∥]*Current address: Department of Optometry and Vision Science, New Zealand National Eye Centre, University of Auckland, Auckland, New Zealand*

Received September 1, 2010; Revised Manuscript Received October 11, 2010

ABSTRACT: Fatty acid acylation of proteins is a well-studied co- or posttranslational modification typically conferring membrane trafficking signals or membrane anchoring properties to proteins. Commonly observed examples of protein acylation include N-terminal myristoylation and palmitoylation of cysteine residues. In the present study, direct tissue profiling mass spectrometry of bovine and human lens sections revealed an abundant signal tentatively assigned as a lipid-modified form of aquaporin-0. LC/MS/MS proteomic analysis of hydrophobic tryptic peptides from lens membrane proteins revealed both N-terminal and C-terminal peptides modified by 238 and 264 Da which were subsequently assigned by accurate mass measurement as palmitoylation and oleoylation, respectively. Specific sites of modification were the N-terminal methionine residue and lysine 238 revealing, for the first time, an oleic acid modification via an amide linkage to a lysine residue. The specific fatty acids involved reflect their abundance in the lens fiber cell plasma membrane. Imaging mass spectrometry indicated abundant acylated AQP0 in the inner cortical region of both bovine and human lenses and acylated truncation products in the lens nucleus. Additional analyses revealed that the lipid-modified forms partitioned exclusively to a detergent-resistant membrane fraction, suggesting a role in membrane domain targeting.

Fatty acid acylation and prenylation of proteins are well-studied, tissue-specific co- or posttranslational modifications that affect protein trafficking and anchoring of membrane-associated proteins or cytoplasmic loops of integral membrane proteins. Classic examples include G-protein coupled receptors and their downstream signaling partners, heterotrimer GTP[1]-binding proteins. In ocular tissues these include Gα-transducin where heterogeneous N-terminal N-acylation (*1*) affects transducin translocation within the photoreceptor (*2*), its affinity for its heterotrimeric partners (*3*), and the kinetics of the photoresponse (*4*). In addition, rhodopsin is doubly palmitoylated at residues Cys322 and Cys323, which serves to anchor the H8 amphipathic helix to the membrane creating an additional binding site for transducin (*5*). While numerous proteins have been shown to be N-terminally acylated, only a small number of proteins have been reported to contain amide-linked palmitic acid or myristic acid modifications on lysine residues. These include palmitoylated lung surfactant protein C (*6*), myristoylated interleukin 1 alpha (IL-1α)(*7*), and myristoylated tumor necrosis factor alpha (TNF-α)(*8*). The mechanism of formation, as well as the functional consequences of this rare modification, remains unknown.

In addition to membrane anchoring, membrane trafficking, and cell signal regulation, fatty acylation of proteins can target proteins within plasma membrane domains, e.g., lipid raft domains (*9*, *10*). Protein localization within or outside of lipid raft domains can significantly affect function. For example, when acylated with unsaturated or polyunsaturated lipids, the Src family kinase member Fyn has reduced localization in lipid rafts resulting in decreased signal transduction in T cells (*10*). Additionally, palmitoylation of aquaporin 4 (AQP4) resulted in inhibition of square array formation in CHO cells (*11*). Although fatty acid modifications to aquaporin-5 (AQP5) have yet to be found, it is known that AQP5 traffics between raft and nonraft membrane domains upon cholinergic stimulation (*12*). Aquaporins-8 and -9 also traffic between membrane domains in hepatocytes (*13*). In the ocular lens, AQP0 has been shown to be present in both detergent-resistant (lipid raft) and detergent-soluble membrane fractions (*14*). In vitro studies have shown AQP0 to be a substrate for Cys palmitoylation (*15*) although conflicting results have been published (*16*).

Aquaporin-0 (AQP0) is the most abundant integral membrane protein in the ocular lens where it functions as a water channel and an adhesion protein (*17*−*21*). Due to loss of fiber cell organelles during differentiation to form a transparent tissue, there is little protein turnover of lens proteins particularly in the deeply buried cells of the aged lens core. Therefore, lens proteins serve as a model for protein aging. With age, AQP0 has been shown to be extensively modified by truncation, phosophorylation,

[†]This work was supported by NIH Grant EY13462 and by Vanderbilt Vision Research Center Grant P30 EY-08126.

*Corresponding author. Phone: 615-936-6861. Fax: 615-343-8372. E-mail: Kevin.schey@vanderbilt.edu.

[1]Abbreviations: ACN, acetonitrile; AQP0, aquaporin-0; AQP2, aquaporin-2; AQP4, aquaporin-4; AQP5, aquaporin-5; Da, dalton; DRM, detergent-resistant membrane fraction; DSM, detergent-soluble membrane fraction; DTT, dithiothreitol; EDTA, ethylenediaminetetraacetic acid; FA, formic acid; GTP, guanine triphosphate; HFIP, hexafluoro-2-propanol; HPLC, high-performance liquid chromatography; IL-1α, interleukin 1 alpha; ITO, indium tin oxide; LC/MS/MS, liquid chromatography tandem mass spectrometry; LRAT, lecithin: retinol acyltransferase; MALDI, matrix-assisted laser desorption ionization; MS/MS, tandem mass spectrometry; NaF, sodium fluoride; NH_4HCO_3, ammonium bicarbonate; PMSF, phenylmethanesulfonyl fluoride; SA, sinapinic acid; TFA, trifluoroacetic acid; TNF-α, tumor necrosis factor alpha.

 Published on Web 10/13/2010

deamidation, and isomerization/racemization (*22*−*24*). An interesting aspect of the unique biochemistry of lens proteins is that posttranslational modification may provide a mechanism to change lens protein function as fiber cells age as an alternative to protein degradation and synthesis of new proteins. This hypothesis has been argued in the case of connexin 50 where C-terminal truncation with fiber cell age removes pH regulation of the gap junction (*25*) and may also be the case where truncated AQP0 becomes the junctional form (*20*). The functional consequences of AQP0 modifications continue to be actively investigated. For example, recent reports demonstrate that phosphorylation alters calmodulin binding (*26*, *27*), a key regulator of AQP0 permeability (*28*, *29*), and predict that C-terminal truncation alters cytoskeletal interactions (*30*).

In this study, direct tissue profiling by mass spectrometry revealed a putative lipid modification to AQP0 in bovine and human tissue that had not been previously observed in standard proteomic studies. By altering proteomic protocols for more hydrophobic peptide analysis, fatty acid modified peptides of AQP0 were observed. Accurate mass measurements and tandem mass spectrometry revealed N-terminal and C-terminal peptides modified by either palmitic acid or oleic acid, the latter of which has not been previously reported in eukaryotic proteins. Imaging mass spectrometry indicates that this modification is formed in the inner cortical region of the lens and can be equal in abundance to unmodified AQP0. Moreover, this fatty acid modified AQP0 is localized exclusively to the detergent-resistant membrane fraction, presumably in lipid raft domains, suggesting that these modifications play a role in membrane localization and potentially in regulating AQP0 function.

MATERIALS AND METHODS

Materials. Frozen bovine lenses were obtained from Pel-Freez Biologicals (Rogers, AR), and frozen human lenses were obtained from NDRI (Philadelphia, PA). Indium tin oxide (ITO) coated conductive glass microscope slides were purchased from Bruker Daltonics (Billerica, MA). Tissue freezing medium (TFM) was obtained from Triangle Biomedical Sciences, Inc. (Durham, NC). All other chemical and biochemical reagents were obtained from Sigma-Aldrich (St. Louis, MO).

Tissue Sectioning. Frozen bovine and human lenses were attached to cold specimen chucks by application of a small amount of TFM embedding medium at the base of the tissue only. Equatorial or axial sections of 20 μm thickness were obtained at −20 °C using a disposable blade stage-equipped cryostat (Leica CM3050 S, Wetzlar, Germany, or Microm HM 550, Walldorf, Germany). To collect frozen sections, a thin, uniform layer of ethanol or methanol was applied at room temperature to a conductive glass slide (tissue profiling) or to a gold-coated MALDI target plate (tissue imaging), and cryosections were thaw-mounted by touching the MALDI target to the tissue section prior to evaporation of solvent. For axial sections, lens polarity was determined using standard hematoxylin and eosin staining of a sister section and identifying the epithelial cell monolayer which covers the lens anterior pole (data not shown).

Direct Tissue Profiling. Profiling of AQP0 from human lens sections was performed as described previously (*31*); however, washing was altered slightly to aid in section adherence to the slide. HPLC grade water (Fisher Scientific, Suwanee, GA), 100−200 μL, was placed on top of the tissue section for 1 min. The water was removed by aspiration, and the section was allowed to dry for 4 min. This was repeated two additional times, and the section was allowed to air-dry completely, after which the entire wash−dry cycle was repeated a second time. Dried tissue sections were spotted manually with ≤0.1 μL of 7:3 formic acid:hexafluoro-2-propanol (FA:HFIP) in specific locations, followed by ≤0.1 μL of saturated sinapinic acid (SA) matrix in 90% acetonitrile (ACN) and 0.1% trifluoroacetic acid (TFA). The sections were analyzed using a Bruker Autoflex III TOF mass spectrometer (Bruker Daltonics, Bremen Germany) in positive ion linear mode, and 350 shots/spectrum were acquired. FlexAnalysis software was used for peak detection; smoothing and baseline subtraction were not utilized. Mass spectra were calibrated using calibration mixture 3 (bovine insulin, *E. coli* thioredoxin, equine apomyoglobin) of the Applied Biosystems Sequazyme peptide mass standards kit (Applied Biosystems, Foster City, CA) or Bruker protein calibration standard 1 (bovine insulin, equine cytochrome *c*, bovine ubiquitin I, equine myoglobin (Bruker Daltonics, Bremen Germany)).

On-Tissue Digestion for Direct Tissue Profiling. Thawed lens sections were covered with ≤250 μL of HPLC grade water, which was aspirated after 1 min of washing. The sections were desiccated completely (*32*) between washes (six total). Each section was washed an additional seven times in a water bath for 1 min with desiccation between washes. Once dry, sections were covered with 10−15 μL of 0.05 μg/μL endoproteinase Lys-C (Roche Applied Science) in 50 mM NH_4HCO_3:ACN (90:10) and incubated for 14 h in a self-constructed humidity chamber. A slightly higher concentration of enzyme has been used previously for on-tissue trypsin digestion (*33*). As a control, sections were also incubated without Lys-C. After the incubation period, sections were quickly rinsed in a water bath for 10 s. Immediately following, the sections were washed three times with a 1 min water bath and desiccated after the final water bath.

Direct Tissue Imaging. Imaging of AQP0 from bovine and human lens sections was performed as described previously (*34*). Following tissue sectioning as described above, sections were washed 10 times by pipetting water onto the sections, incubating for 1 min, removing excess water by pipet, and desiccating sections until remaining water had evaporated. After washing, automated matrix deposition was carried out using a Portrait 630 acoustic reagent multispotter (Labcyte Inc., Sunnyvale, CA). Forty passes of one spot (170 pL) per pass of 20 mg/mL sinapinic acid in 90% ACN/0.2% TFA were applied with a center-to-center spot distance of 300 μm for bovine lenses. For human lenses, four arrays with a center-to-center spot distance of 400 μm were applied successively, shifting each array 200 μm in *x* and/or *y* to create an array of matrix spots with a center-to-center spot distance of 200 μm. Mass spectrometric analyses were performed in the linear, positive mode at +20 kV accelerating potential on a time-of-flight mass spectrometer (Bruker Autoflex II Linear; Bruker Daltonics, Bremen, Germany), which was equipped with a Smartbeam laser operating at a repetition rate of 200 Hz. Delayed extraction parameters were optimized for signal intensity and mass resolution at a focus mass of 28 kDa. A linear, external calibration was applied to the instrument prior to data collection using a protein mixture of insulin ($M + H^+ = 5734$), cytochrome *c* ($M + H^+ = 12361$), myoglobin ($M + H^+ = 16952$), and trypsinogen ($M + H^+ = 23982$). Mass spectral data sets were acquired over lens sections with a raster step size of 200−300 μm and 300 laser shots per spectrum using flexImaging software (Bruker Daltonics, Bremen, Germany). After data acquisition, molecular images were reconstituted using the

flexImaging software. Data were normalized to total ion current using flexImaging software, and each m/z signal was plotted ± 0.15% mass-to-charge units. MALDI images are displayed using interpolation, which applies a linear gradient of pixel intensity change between adjacent sampling locations for each plotted m/z signal.

LC/MS/MS. (*A*) *Lens Membrane Preparation*. Lens membrane proteins were prepared from whole lens homogenates as previously described (*22*). Briefly, frozen bovine or human lenses were decapsulated and dissected into cortex and nucleus regions prior to homogenization. Tissue was manually homogenized in 50 mM ammonium bicarbonate buffer containing 5 mM EDTA, 10 mM NaF, 1 mM DTT, and 1 mM PMSF, pH 8, and centrifuged at 20000*g* for 30 min. The supernatant was discarded, and the pellets were washed three times with 50 mM ammonium bicarbonate buffer containing 8 M urea, 5 mM EDTA, 10 mM NaF, 1 mM DTT, and 1 mM PMSF, pH 8, followed by triplicate water washes. The remaining pellets were reduced and alkylated by incubating the pellets for 1 h at 56 °C with 10 mM DTT followed by 45 min incubation with 55 mM iodoacetamide at room temperature in the dark. The excess reagents were removed by triplicate water washes of the pellets.

(*B*) *Detergent Extraction Methods*. The pellets were disrupted periodically by a hand-held homogenizer in 500 μL of freshly prepared TNE buffer (25 mM Tris, 150 mM NaCl, 5 mM EDTA, pH 7.5) containing 1% Triton X-100 on ice for 40 min. After centrifugation at 193800 g the supernatants were collected as detergent-soluble membrane fractions (DSM), and the remaining pellets were collected as detergent-resistant membrane fractions (DRM). To remove Triton, the volume of the DSM fraction was reduced to about 100 μL by Speedvac, and the DRM fraction was resuspended in 100 μL of Milli-Q water. Then, 900 μL of ice-cold acetone was added, and the samples were incubated at −20 °C for 30 min. Precipitated proteins were pelleted by centrifugation at 193800*g*, and pellets were washed twice with Milli-Q water.

(*C*) *Trypsin Digestion*. Pelleted proteins were suspended in 50 mM ammonium bicarbonate buffer and digested by trypsin for 20 h at 37 °C. Trypsin digests were dried in a SpeedVac, and the peptides were reconstituted in 0.1% TFA and centrifuged at 124300*g* for 10 min. The supernatant was removed, and the pellets were washed with 0.1% TFA again. The remaining pellets were extracted twice with 95% acetonitrile (ACN) (0.1% TFA), and the extracts were pooled, dried, and subsequently reconstituted in 5% ACN (0.1% formic acid) for LC/MS/MS analysis.

(*D*) *LC/MS/MS*. Peptides were separated on a fused silica capillary column (150 mm × 100 μm) packed in-house with Phenomenex Jupiter resin (5 μm mean particle size, 300 Å pore size). HPLC separation was performed using the following gradient: 0−2 min, 2−5% ACN (0.1% formic acid); 2−45 min, 5−100% ACN (0.1% FA); 45−50 min, 100% ACN (0.1% FA) at a flow rate of 0.5 μL/min. The eluate was directly infused into a LTQ, LTQ-Orbitrap, or Velos mass spectrometer (ThermoFisher, San Jose, CA) with a nanoelectrospray source. MS scans were acquired in LTQ-Orbitrap with a mass resolving power of 60000. Data acquisition was carried out in both targeted mode and data-dependent mode with the top four most abundant ions in each MS scan. MS^3 was also performed in the LTQ by selection of the m/z 910.7 fragment of the m/z 1007.0 parent ion and the m/z 897.6 fragment of the m/z 998.0 parent ion. Tandem mass spectra were manually interpreted.

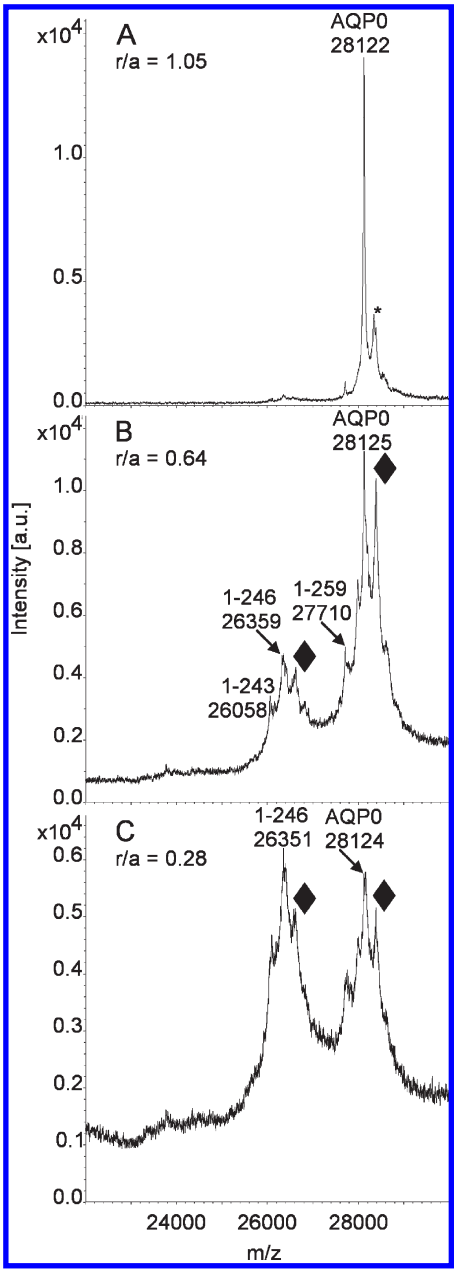

FIGURE 1: Direct tissue profiling of lens membrane protein AQP0. MALDI mass spectra acquired directly from a 29-year-old human lens section indicate that the ~264 Da modification (labeled with a black diamond) is not apparent in the outer cortex (A), but its presence increases abundantly in the nucleus region (B) and remains in the outer core (C). The asterisk represents a sinapinic acid matrix adduct, shifted by 206 Da. Note that an r/a of 1.05 in panel A corresponds to the center of the matrix spot being outside of the tissue but that the matrix spot covers the tissue edge (outer cortex).

RESULTS

Using a recently developed method for direct tissue profiling of integral membrane proteins (*31*) both bovine and human lens tissue sections revealed an abundant signal at approximately 264 Da higher in molecular mass than unmodified AQP0 (predicted MH^+ ion, m/z 28123). This putative modified form of AQP0 was not evident in the outer cortical region (r/a = 1.05, where r is the radial distance of the sampling location from the center of the lens section and a is the radius of the lens section) of a 29-year-old human lens (Figure 1A) but is nearly equal in abundance to unmodified AQP0 in the outer nucleus region (r/a of 0.64) (Figure 1B). Moving inward toward the lens core, the modification

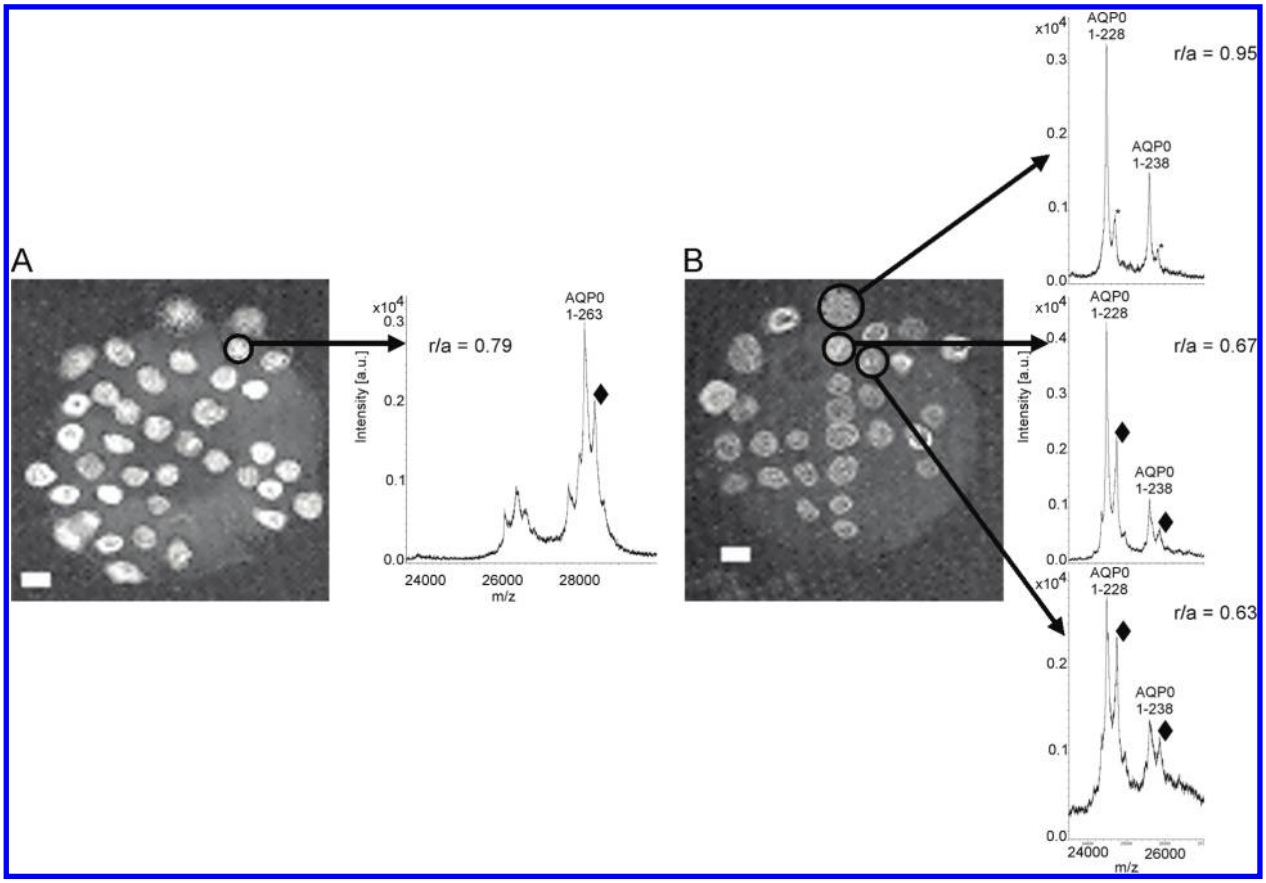

FIGURE 2: Direct tissue profiling after on-tissue Lys-C digestion of AQP0. Lens sections were incubated (A) without or (B) with Lys-C for 14 h. Representative spectra from different locations within the lens show the distribution of the putative C18:1 lipid modification (represented by black diamonds, ♦) on intact AQP0 (A) and the N-terminal fragments of AQP0 (B). r/a = normalized lens distance; * = sinapinic acid matrix adduct. Scale bar = 1 mm.

appears to be present on the major AQP0 truncation product, AQP0 1−246 (predicted MH^+ ion, m/z 26359) (Figure 1C), suggesting that the predominant site of modification is not in the distal C-terminal region (residues 247−263). Furthermore, in the inner cortex and nuclear regions it appears that the abundance of modified AQP0 is nearly equal to that of the unmodified AQP0. This modified form of AQP0 is observed in all human lenses analyzed (aged 7 to 69), with the same regional distribution as seen in Figure 1 (data not shown). Although it is difficult to obtain a highly accurate mass measurement from these spectra, the mass shift observed for the modified protein suggests a possible fatty acid modification.

On tissue digestion with endoproteinase Lys-C was employed to verify that the observed mass shift was present on predicted APQ0 peptides and that the signal was not due to another protein present in the preparation. The expected proteolytic fragments, 1−238 and 1−228, appeared in the tissue profiles from the outer cortex region (Figure 2B, top panel); however, only sinapinic acid matrix adducts to AQP0 were observed in this region. The spectra from the outer nuclear region (Figure 2B, middle and bottom panels) revealed modified forms of each Lys-C fragment of AQP0 at +264 Da, providing further evidence that these signals arise from AQP0. These data indicate abundant modification on the N-terminal portion (1−228) of AQP0 in near equal amount to that seen for intact AQP0 (Figure 2A).

Standard LC/MS/MS proteomic analysis methods of tryspin-digested lens membrane preparations indicated signals for residues 234−259 of AQP0 in bovine lens and residues 234−263 of AQP0 in human lens that were shifted by +265 and +239 Da. The modified peptides eluted with high organic solvent, which is consistent with the assumption of fatty acid modifications. Given the observed hydrophobicity of the modified peptides and the putative assignment as a fatty acid modification, the pellet of digested protein remaining after aqueous buffer extraction was further extracted with 95% acetonitrile and analyzed. The results indicated that most of the putative lipid-modified peptides remained in the pellet after aqueous buffer extraction

Table 1: Predicted and Observed Masses of Modified Bovine and Human AQP0 Peptides

peptide	modification	predicted MW[a,b]	observed MW[c]
h1−5	none	734.365	734.364
	C18:1	998.611	998.608
	C16:0	972.595	972.592
h234−263	none	3090.632[a]	not measured
	deamidation	3092.600[b]	3092.598
	C18:1	3356.845[b]	3356.829
	C16:0	3330.829[b]	3330.816
b1−5	none	734.365	not measured
	C18:1	998.611	998.605
	C16:0	972.595	972.590
b234−259	none	2752.436[b]	not measured
	C18:1	3016.682[b]	3016.666
	C16:0	2990.666[b]	2990.654

[a]Monoisotopic masses. [b]Includes deamidation. [c]Accurate mass measurement using Orbitrap.

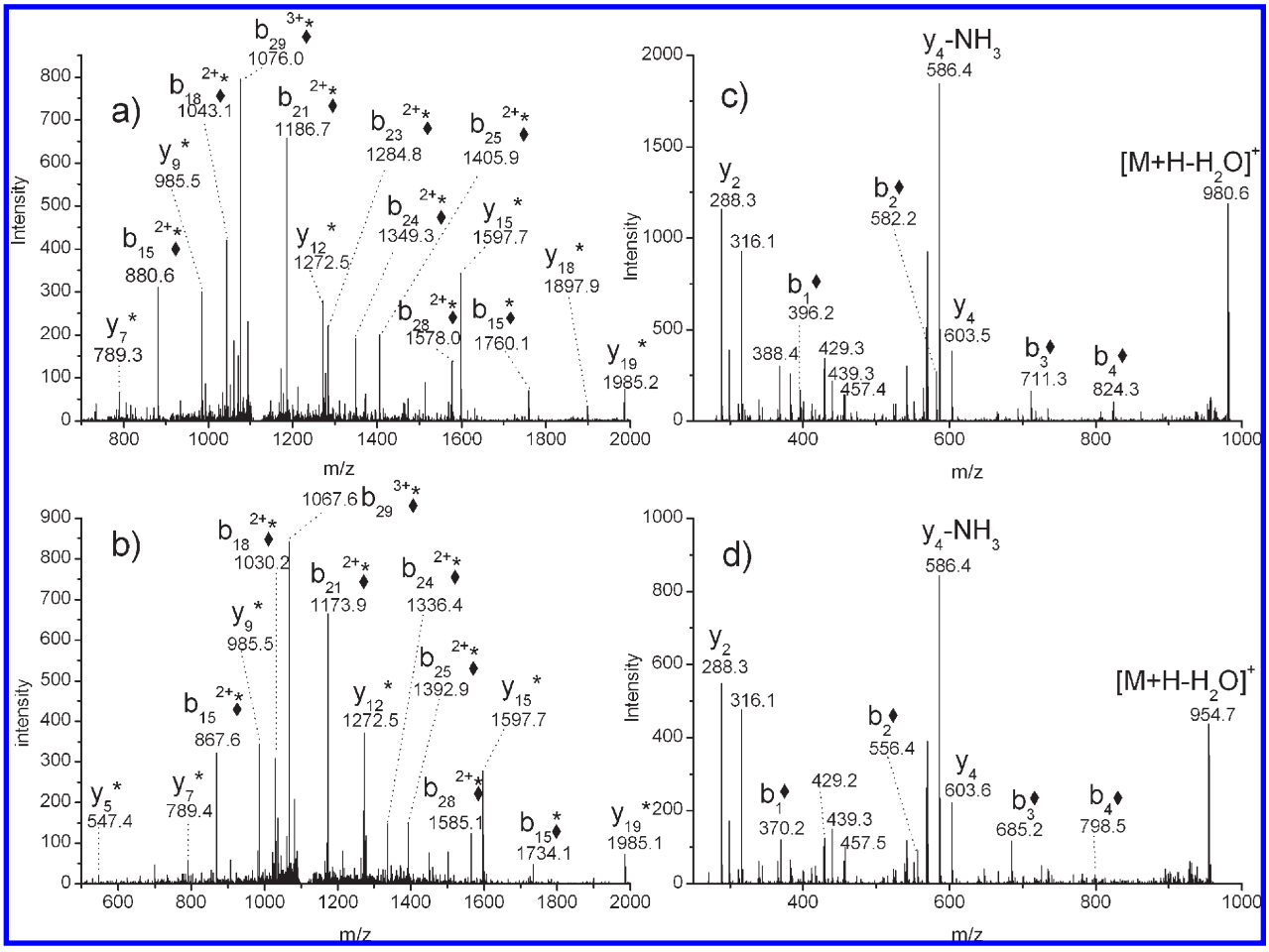

FIGURE 3: Tandem mass spectra of modified human AQP0 peptides. Tandem mass spectrum of (a) AQP0 234−263 modified by oleic acid ($[M + 3H]^{3+}$, m/z 1119.2), (b) AQP0 234−263 modified by palmitic acid ($[M + 3H]^{3+}$, m/z 1110.5), (c) AQP0 1−5 modified by oleic acid ($[M + H]^+$, m/z 998.6), and (d) AQP0 1−5 modified by palmitic acid ($[M + H]^+$, m/z 973.2). Black diamonds (♦) indicate fragment ions shifted in mass by lipid modification. Asterisks indicate fragment ions shifted in mass by deamidation. AQP0 234−263 sequence: LSVLK♦GAKPDVSN*GQPEVTGEPVELN*TQAL. AQP0 1−5 sequence: ♦MWELR.

and that the modified peptides were enriched by acetonitrile extraction of the remaining pellet. Analysis of the organic extract of the pellet revealed several AQP0 peptides modified by +265 and +239 Da such as residues 234−259 of bovine AQP0, residues 234−263 of human AQP0, and truncated peptides 234−259 and 234−246 in human lens. The analysis also revealed that the N-terminal peptide 1−5 of AQP0 was modified by +264 and +238 Da in both bovine and human lens samples. Accurate mass measurements using an Orbitrap mass spectrometer revealed mass shifts of 265.192 and 239.180 to AQP0 234−259 and 264.234 and 238.219 to AQP0 1−5 in bovine lens and mass shifts of 266.197 and 240.184 to AQP0 234−263 and 264.243 and 238.227 to AQP0 1−5 in human lens (Table 1). The N-terminal mass shifts are consistent with palmitic acid (C16:0) and oleic acid (C18:1) modifications, and C-terminal mass shifts in bovine lens are consistent with palmitic acid and oleic acid modifications with the additional one mass unit shift on the C-terminal peptide due to deamidation of asparagine 246, commonly observed in older lens fiber cells. The C-terminal mass shifts for human AQP0 peptide 234−263 are consistent with two deamidations at asparagine residues 246 and 259 commonly observed in older human lenses (*35*). Note that no double bond assignment can be made based on the tandem mass spectral information; however, since oleic acid is the most abundant C18:1 lipid in the lens, the most likely 264 Da modification is oleoylation.

Tandem mass spectra of modified human AQP0 234−263 ($[M + 3H]^{3+}$ ions selected) indicate that all observed b-ions (b_{15} and above) are modified by either 264 Da (Figure 3a) or 238 Da (Figure 3b) whereas y-ions are modified only by deamidation. Since the b-ion nomenclature dictates that b-ions contain the peptide N-terminus, these results suggest that the lipid modifications are present within the first 15 residues of this peptide. The sites of deamidation are Asn246 and Asn259 as reported previously (*35*). Selection and further fragmentation (MS^3) of the major b-ion, b_{15}^{2+}, from modified bovine lens AQP0 234−259 indicates that the site of modification is lysine 238 (Supporting Information Figure 1). The attachment of the lipid moieties, therefore, is via an amide linkage to the lysine amino group, a known structure for palmitic acid modified lysine residues and novel for oleic acid modified lysine residues. Tandem mass spectra of modified AQP0 1−5 peptides indicate that all N-terminal containing b-ions are shifted by 264 Da (Figure 3c) or 238 Da (Figure 3d). Moreover, no y-ions were observed as shifted in mass, indicating that the site of modification is the N-terminal amino group.

Given the previous finding that AQP0 distributes in both detergent-soluble (DSM) and detergent-resistant (DRM) lens membrane fractions (*14*), we tested the hypothesis that lipid modification to AQP0 could target AQP0 to the detergent-resistant (lipid raft)

fraction. Mass spectrometry analysis of DRM and DSM fractions revealed that, although unmodified AQP0 peptides were detected in both DRM and DSM fractions, palmitic acid and oleic acid modified AQP0 peptides were exclusively detected in the DRM fraction (Figure 4). Both N-terminal and C-terminal modified peptides were detected in the DRM fraction only, and, consistent with on-tissue digestion results (Figure 2), the N-terminal modification appears to be more abundant that the C-terminal modification.

A recently developed method for direct tissue imaging of integral membrane proteins (*34*) was applied to lens tissue sections in an effort of view the spatial distribution of modified AQP0. Figure 5 shows the images of unmodified full-length AQP0 (Figure 5A−C) and the oleic acid modified form of full-length AQP0 (Figure 5D−F) acquired directly from bovine and human lens sections. As expected from previous work, full-length, unmodified AQP0 is detected in the outer cortical region of bovine equatorial and axial sections (panels A and B of Figure 5, respectively) at the predicted m/z 28224 ± 0.07% and in 11-year-old human equatorial sections (Figure 5C) at the predicted m/z 28123 ± 0.02%. Interestingly, the fatty acylated (oleic acid) AQP0 signal detected at the predicted m/z 28489 ± 0.14% (bovine, Figure 5D) and at the predicted m/z 28388 ± 0.04% (human, Figure 5F) is most abundant in the inner cortical and outer nuclear region of both species, which is in agreement with the direct tissue profiling results presented in Figure 1. Note that the instrumentation used cannot resolve different lipidated species at the intact protein mass; however, oleic acid is the most abundant species observed (Figure 4), and the measured mass is closest to this modified form of AQP0. No anterior−posterior differences are observed in the bovine lens (Figure 5E). The decrease of the fatty acid modified signal is due to truncation of the full-length AQP0; however, the truncated AQP0 products retain the modification as seen in the profiling data (Figure 1).

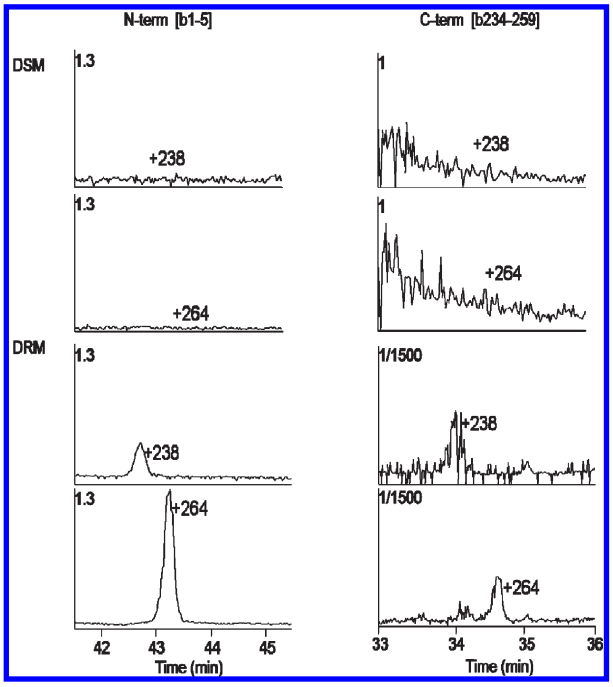

FIGURE 4: Mass spectrometry of bovine AQP0 peptides in DRM and DSM fractions. Selected ion chromatograms of modified AQP0 1−5 (left column) and AQP0 234−259 (right column) peptides from detergent-soluble (top panels) and detergent-resistant (bottom panels) membrane fractions. All signals were normalized to the intensity of unmodified AQP0 peptide 188−196, present in both DRM and DSM samples. The normalization factor used to plot each signal is located in the upper left of each chromatogram.

DISCUSSION

Two fatty acid modifications, one rare and one novel, have been identified in high abundance on the major lens membrane protein AQP0 in both bovine and human lenses. In addition, two sites of modification were discovered, the predominant one on the N-terminal methionine and one on a C-terminal lysine residue, Lys238. Lysine modification by palmitic acid is relatively rare while modification by oleic acid has not been previously reported. Direct tissue profiling and imaging methods reveal that these modifications are present in a spatially distinct region (outer nucleus and core) and are present in significant abundance, nearly equal to unmodified AQP0. The distinct distribution of acylated forms of AQP0 suggests that the modification occurs at a specific time during lens maturation, that is, in a programmed fashion. Recently, homogenates from fetal lenses were profiled, revealing that the modification is not present in the fetal lens (*23*).

To date, only a few eukaryotic proteins have been identified with amide-linked fatty acid modifications on lysine residues. The mechanism of formation and the functional significance of this modification remain unknown. It has been suggested that this modification is a result of residence time in the lipid membrane environment (*36*) perhaps by nucleophilic addition of the fatty acid to available amino groups. This putative mechanism would be particularly applicable to very long lived lens proteins, and it is noteworthy that the two fatty acids observed on AQP0 correspond to the two most abundant fatty acids in the lens plasma membrane (*37*). An extension of this concept is that nervonic acid (C24:1), the third most abundant fatty acid present in human lens membranes, would be expected to be present on AQP0. This specific modification has not been detected in the present study, either because it is not formed or because of the extreme hydrophobicity of this lipid preventing extraction during sample preparation or elution from the C18 column during peptide separation. More interesting perhaps is the notion that if the aforementioned mechanism is correct, many integral membrane proteins of the lens could be modified in similar ways although none have been detected to date. Additionally, the functional consequences could be significant. An alternative mechanism could be that an, as yet unidentified, acyltransferase enzyme is responsible for placing this lipid modification on the protein. The specificity of fatty acids involved would be determined by the transferase as is reported for lecithin:retinol acyltransferase (LRAT) (*38*).

As described in the introduction, N-terminal acylation is a well-studied modification that plays a role in membrane trafficking, membrane domain targeting, and protein−protein interactions. Moreover, specific protein functions can be altered, as is the case for transducin in the visual signal transduction cascade. To date, no evidence exists for AQP0 shuttling as is observed for AQP2 in the collecting duct of the kidney in response to vasopressin (*39*); i.e., all AQP0 traffics directly to the fiber cell plasma membrane. Since outer cortical AQP0 is devoid of lipid modifications, membrane trafficking is not likely affected by this modification.

The presence of lipid-modified AQP0 in detergent-resistant membrane fractions suggests that this modification targets AQP0 to different membrane domains, i.e., that fatty acylated AQP0 resides in detergent-resistant, lipid raft domains while unmodified

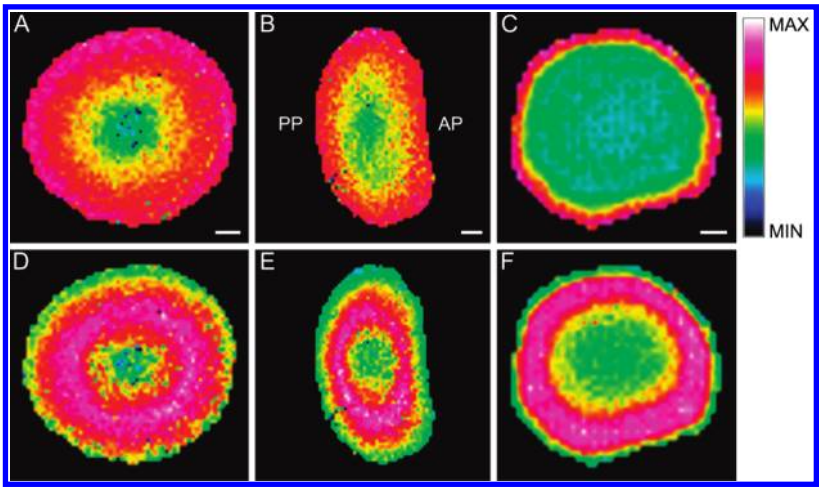

FIGURE 5: MALDI imaging of unmodified and fatty acylated full-length AQP0 in bovine and human lenses. Unmodified full-length AQP0 is most abundant in the cortex of (A) equatorial bovine (observed m/z 28203), (B) axial bovine (observed m/z 28220), and (C) equatorial 11-year-old human (observed m/z 28126) lenses. Full-length AQP0 modified with oleic acid is most abundant in the lens inner cortex and outer nucleus of (D) equatorial bovine (observed m/z 28420), (E) axial bovine (observed m/z 28448), and (F) equatorial 11-year-old human (observed m/z 28377) lenses. No anterior−posterior variation is observed in the bovine lens. Scale bars: bovine equatorial, bovine axial, and human equatorial = 2, 2, and 1 mm, respectively.

AQP0 resides in nonlipid raft regions of the plasma membrane. At this point, it is unclear what functional roles AQP0 plays in different membrane environments; however, it is clear from previous work that AQP0 exists in different membrane environments within a single elongated fiber cell (*40*) and changes its membrane distribution in progressively older, more deeply buried lens fiber cells (*41*). AQP0 is a major component of lens membrane square arrays and also is present at the periphery of lens gap junctions (*42*−*44*). Lenses deficient in AQP0 are devoid of interlocking membrane structures, square arrays, and have increased gap junction areas (*45*). Although palmitoylation of AQP4 inhibits square array formation (*11*), the role of fatty acylated AQP0 in different lens membrane structures remains to be determined.

Lipid modification of AQP0 in the outer nuclear region could represent another example of altered protein function via post-translational modification in the aging lens. Besides a membrane targeting function, it is possible that fatty acid acylation of the C-terminal lysine 238 residue could anchor the C-terminal cytoplasmic tail to the lipid membrane providing access to binding partners. Note that in published AQP0 structures (*46*, *47*) the α-helical C-terminal tail lies parallel to the plane of the plasma membrane. Alternatively, one must consider that the modified lysine residue lies within the demonstrated calmodulin binding site and could affect this protein−protein interaction that regulates channel permeability. Given the importance of the C-terminal tail in regulating AQP0 permeability and possibly membrane−cytoskeletal interactions, it seems likely that an abundant modification in this region would have significant functional consequences.

ACKNOWLEDGMENT

The authors acknowledge use of the Mass Spectrometry Facility at the Medical University of South Carolina and the Proteomics Core Facility in the Mass Spectrometry Research Center at Vanderbilt University.

SUPPORTING INFORMATION AVAILABLE

One figure showing mass spectra of oleic acid modified bovine AQP0 234−259 indicating the exact site of modification. This material is available free of charge via the Internet at http://pubs.acs.org.

REFERENCES

1. Neubert, T. A., and Hurley, J. B. (1998) Functional heterogeneity of transducin alpha subunits. *FEBS Lett. 422*, 343–345.
2. Lobanova, E. S., Finkelstein, S., Song, H., Tsang, S. H., Chen, C. K., Sokolov, M., Skiba, N. P., and Arshavsky, V. Y. (2007) Transducin translocation in rods is triggered by saturation of the GTPase-activating complex. *J. Neurosci. 27*, 1151–1160.
3. Kokame, K., Fukada, Y., Yoshizawa, T., Takao, T., and Shimonishi, Y. (1992) Lipid modification at the N terminus of photoreceptor G-protein alpha-subunit. *Nature 359*, 749–752.
4. Kerov, V., Rubin, W. W., Natochin, M., Melling, N. A., Burns, M. E., and Artemyev, N. O. (2007) N-terminal fatty acylation of transducin profoundly influences its localization and the kinetics of photoresponse in rods. *J. Neurosci. 27*, 10270–10277.
5. Sakmar, T. P. (2002) Structure of rhodopsin and the superfamily of seven-helical receptors: the same and not the same. *Curr. Opin. Cell Biol. 14*, 189–195.
6. Gustafsson, M., Curstedt, T., Jornvall, H., and Johansson, J. (1997) Reverse-phase HPLC of the hydrophobic pulmonary surfactant proteins: detection of a surfactant protein C isoform containing Nepsilon-palmitoyl-lysine. *Biochem. J. 326* (Patt 3), 799–806.
7. Stevenson, F. T., Bursten, S. L., Fanton, C., Locksley, R. M., and Lovett, D. H. (1993) The 31-kDa precursor of interleukin 1 alpha is myristoylated on specific lysines within the 16-kDa N-terminal propiece. *Proc. Natl. Acad. Sci. U.S.A. 90*, 7245–7249.
8. Stevenson, F. T., Bursten, S. L., Locksley, R. M., and Lovett, D. H. (1992) Myristyl acylation of the tumor necrosis factor alpha precursor on specific lysine residues. *J. Exp. Med. 176*, 1053–1062.
9. Resh, M. D. (2006) Trafficking and signaling by fatty-acylated and prenylated proteins. *Nat. Chem. Biol. 2*, 584–590.
10. Liang, X., Nazarian, A., Erdjument-Bromage, H., Bornmann, W., Tempst, P., and Resh, M. D. (2001) Heterogeneous fatty acylation of Src family kinases with polyunsaturated fatty acids regulates raft localization and signal transduction. *J. Biol. Chem. 276*, 30987–30994.
11. Suzuki, H., Nishikawa, K., Hiroaki, Y., and Fujiyoshi, Y. (2008) Formation of aquaporin-4 arrays is inhibited by palmitoylation of N-terminal cysteine residues. *Biochim. Biophys. Acta 1778*, 1181–1189.
12. Ishikawa, Y., Yuan, Z., Inoue, N., Skowronski, M. T., Nakae, Y., Shono, M., Cho, G., Yasui, M., Agre, P., and Nielsen, S. (2005) Identification of AQP5 in lipid rafts and its translocation to apical membranes by activation of M3 mAChRs in interlobular ducts of rat parotid gland. *Am. J. Physiol. Cell. Physiol. 289*, C1303–C1311.
13. Mazzone, A., Tietz, P., Jefferson, J., Pagano, R., and LaRusso, N. F. (2006) Isolation and characterization of lipid microdomains from apical and basolateral plasma membranes of rat hepatocytes. *Hepatology 43*, 287–296.

14. Tong, J., Briggs, M. M., Mlaver, D., Vidal, A., and McIntosh, T. J. (2009) Sorting of lens aquaporins and connexins into raft and nonraft bilayers: role of protein homo-oligomerization. *Biophys. J. 97*, 2493–2502.
15. Manenti, S., Dunia, I., and Benedetti, E. L. (1990) Fatty acid acylation of lens fiber plasma membrane proteins. MP26 and alpha-crystallin are palmitoylated. *FEBS Lett. 262*, 356–358.
16. Cenedella, R. J. (1990) Palmitoylation of ocular lens membrane proteins. *Invest. Ophthalmol. Visual Sci. 31*, 368–373.
17. Chandy, G., Zampighi, G. A., Kreman, M., and Hall, J. E. (1997) Comparison of the water transporting properties of MIP and AQP1. *J. Membr. Biol. 159*, 29–39.
18. Varadaraj, K., Kushmerick, C., Baldo, G. J., Bassnett, S., Shiels, A., and Mathias, R. T. (1999) The role of MIP in lens fiber cell membrane transport. *J. Membr. Biol. 170*, 191–203.
19. Michea, L. F., Andrinolo, D., Ceppi, H., and Lagos, N. (1995) Biochemical evidence for adhesion-promoting role of major intrinsic protein isolated from both normal and cataractous human lenses. *Exp. Eye Res. 61*, 293–301.
20. Gonen, T., Cheng, Y., Kistler, J., and Walz, T. (2004) Aquaporin-0 membrane junctions form upon proteolytic cleavage. *J. Mol. Biol. 342*, 1337–13345.
21. Kumari, S. S., and Varadaraj, K. (2009) Intact AQP0 performs cell-to-cell adhesion. *Biochem. Biophys. Res. Commun. 390*, 1034–1039.
22. Ball, L. E., Garland, D. L., Crouch, R. K., and Schey, K. L. (2004) Post-translational modifications of aquaporin 0 (AQP0) in the normal human lens: spatial and temporal occurrence. *Biochemistry 43*, 9856–9865.
23. Korlimbinis, A., Berry, Y., Thibault, D., Schey, K. L., and Truscott, R. J. (2009) Protein aging: truncation of aquaporin 0 in human lens regions is a continuous age-dependent process. *Exp. Eye Res. 88*, 966–973.
24. Grey, A. C., and Schey, K. L. (2009) Age-related changes in the spatial distribution of human lens alpha-crystallin products by MALDI imaging mass spectrometry. *Invest. Ophthalmol. Visual Sci. 50*, 4319–4329.
25. Lin, J. S., Eckert, R., Kistler, J., and Donaldson, P. (1998) Spatial differences in gap junction gating in the lens are a consequence of connexin cleavage. *Eur. J. Cell Biol. 76*, 246–250.
26. Reichow, S. L., and Gonen, T. (2008) Noncanonical binding of calmodulin to aquaporin-0: implications for channel regulation. *Structure 16*, 1389–1398.
27. Rose, K. M., Wang, Z., Magrath, G. N., Hazard, E. S., Hildebrandt, J. D., and Schey, K. L. (2008) Aquaporin 0-calmodulin interaction and the effect of aquaporin 0 phosphorylation. *Biochemistry 47*, 339–347.
28. Nemeth-Cahalan, K. L., and Hall, J. E. (2000) pH and calcium regulate the water permeability of aquaporin 0. *J. Biol. Chem. 275*, 6777–6782.
29. Varadaraj, K., Kumari, S., Shiels, A., and Mathias, R. T. (2005) Regulation of aquaporin water permeability in the lens. *Invest. Ophthalmol. Visual Sci. 46*, 1393–1402.
30. Lindsey Rose, K. M., Gourdie, R. G., Prescott, A. R., Quinlan, R. A., Crouch, R. K., and Schey, K. L. (2006) The C terminus of lens aquaporin 0 interacts with the cytoskeletal proteins filensin and CP49. *Invest. Ophthalmol. Visual Sci. 47*, 1562–1570.
31. Thibault, D. B., Gillam, C. J., Grey, A. C., Han, J., and Schey, K. L. (2008) MALDI tissue profiling of integral membrane proteins from ocular tissues. *J. Am. Soc. Mass Spectrom. 19*, 814–822.
32. Grey, A., Chaurand, P., Caprioli, R., and Schey, K. (2009) MALDI imaging mass spectrometry of integral membrane proteins from ocular lens and retinal tissue. *J Proteome Res. 8*, 3278–3283.
33. Groseclose, M. R., Andersson, M., Hardesty, W. M., and Caprioli, R. M. (2007) Identification of proteins directly from tissue: in situ tryptic digestions coupled with imaging mass spectrometry. *J. Mass Spectrom. 42*, 254–262.
34. Grey, A. C., Chaurand, P., Caprioli, R. M., and Schey, K. L. (2009) MALDI imaging mass spectrometry of integral membrane proteins from ocular lens and retinal tissue. *J. Proteome Res. 8*, 3278–3283.
35. Schey, K. L., Little, M., Fowler, J. G., and Crouch, R. K. (2000) Characterization of human lens major intrinsic protein structure. *Invest. Ophthalmol. Visual Sci. 41*, 175–182.
36. Johansson, J. (1998) Structure and properties of surfactant protein C. *Biochim. Biophys. Acta 1408*, 161–172.
37. Li, L. K., So, L., and Spector, A. (1987) Age-dependent changes in the distribution and concentration of human lens cholesterol and phospholipids. *Biochim. Biophys. Acta 917*, 112–120.
38. Golczak, M., and Palczewski, K. (2010) An acyl-covalent enzyme intermediate of lecithin:retinol acyltransferase. *J. Biol. Chem. 285*, 29217–29222.
39. Noda, Y., and Sasaki, S. (2005) Trafficking mechanism of water channel aquaporin-2. *Biol. Cell 97*, 885–892.
40. Zampighi, G. A., Eskandari, S., Hall, J. E., Zampighi, L., and Kreman, M. (2002) Micro-domains of AQP0 in lens equatorial fibers. *Exp. Eye Res. 75*, 505–519.
41. Grey, A. C., Li, L., Jacobs, M. D., Schey, K. L., and Donaldson, P. J. (2009) Differentiation-dependent modification and subcellular distribution of aquaporin-0 suggests multiple functional roles in the rat lens. *Differentiation 77*, 70–83.
42. Costello, M. J., McIntosh, T. J., and Robertson, J. D. (1989) Distribution of gap junctions and square array junctions in the mammalian lens. *Invest. Ophthalmol. Visual Sci. 30*, 975–989.
43. Zampighi, G. A., Hall, J. E., Ehring, G. R., and Simon, S. A. (1989) The structural organization and protein composition of lens fiber junctions. *J. Cell Biol. 108*, 2255–2275.
44. Dunia, I., Recouvreur, M., Nicolas, P., Kumar, N., Bloemendal, H., and Benedetti, E. L. (1998) Assembly of connexins and MP26 in lens fiber plasma membranes studied by SDS-fracture immunolabeling. *J. Cell Sci. 111* (Part 15), 2109–2120.
45. Al-Ghoul, K. J., Kirk, T., Kuszak, A. J., Zoltoski, R. K., Shiels, A., and Kuszak, J. R. (2003) Lens structure in MIP-deficient mice. *Anat. Rec., Part A 273*, 714–730.
46. Gonen, T., Sliz, P., Kistler, J., Cheng, Y., and Walz, T. (2004) Aquaporin-0 membrane junctions reveal the structure of a closed water pore. *Nature 429*, 193–197.
47. Harries, W. E., Akhavan, D., Miercke, L. J., Khademi, S., and Stroud, R. M. (2004) The channel architecture of aquaporin 0 at a 2.2-Å resolution. *Proc. Natl. Acad. Sci. U.S.A. 101*, 14045–14050.